Filefish-Inspired Surface Design for Anisotropic Underwater Oleophobicity

Yue Cai, Ling Lin, Zhongxin Xue, Mingjie Liu, Shutao Wang, and Lei Jiang**

Surfaces with anisotropic wettability, widely found in nature, have inspired the development of one-dimensional water control on surfaces relying on the well-arranged surface features. Controlling the wetting behavior of organic liquids, especially the motion of oil fluid on surfaces, is of great importance for a broad range of applications including oil transportation, oil-repellent coatings, and water/oil separation. However, anisotropic oil-wetting surfaces remain unexplored. Here, the unique skin of a filefish *Navodon septentrionalis* shows anisotropic oleophobicity under water. On the rough skin of *N. septentrionalis*, oil droplets tend to roll off in a head-to-tail direction, but pin in the opposite direction. This pronounced wetting anisotropy results from the oriented hook-like spines arrayed on the fish skin. It inspires further exploration of the artificial anisotropic underwater oleophobic surfaces: By mimicking the oriented hook-like microstructure on a polydimethylsiloxane layer via soft lithography and subsequent oxygen-plasma treatment to make the PDMS hydrophilic, artificial fish skin is fabricated which has similar anisotropic underwater oleophobicity. Drawn from the processing of artificial fish skin, a simple principle is proposed to achieve anisotropic underwater oleophobicity by adjusting the hydrophilicity of surface composition and the anisotropic microtextures. This principle can guide the simple mass manufacturing of various inexpensive high surface-energy materials, and the principle is demonstrated on commercial cloth corduroy. This study will profit broad applications involving low-energy, low-expense oil transportation, underwater oil collection, and oil-repellant coatings on ship hulls and oil pipelines.

Dr. Y. Cai, Dr. L. Lin, Dr. Z. Xue, Dr. M. Liu,
Prof. S. T. Wang, Prof. L. Jiang
Beijing National Laboratory for
Molecular Sciences (BNLMS)
Key Laboratory of Organic Solids
Institute of Chemistry
Chinese Academy of Sciences
Beijing 100190, PR China
E-mail: stwang@iccas.ac.cn

Prof. L. Jiang
School of Chemistry and Environment
Beihang University
Beijing, 100191, PR China
E-mail: jianglei@iccas.ac.cn

Dr. Y. Cai, Dr. L. Lin, Dr. Z. Xue, Dr. M. Liu
Graduate School of Chinese Academy of Sciences
Beijing, 100049, PR China

Dr. L. Lin
The Third Institute of Oceanography of the State Oceanic Administration
Xiamen, 361005, China

DOI: 10.1002/adfm.201302034

1. Introduction

Controlling liquid wetting and spreading on solid surfaces has long been an important topic for materials science, receiving remarkable attention from both fundamental research and technological applications including lubrication,[1] coatings,[2] inkjet printing,[3] self-cleaning surfaces,[4] and microfluidics.[5] After years of efforts, it has been revealed that surface wetting behavior is determined by the surface free energy and is further enhanced by micro/nanoscale topographical features. With controlled arrangement of the chemical and structural features, liquids can be driven inhomogeneously on surfaces, enabling the control of droplet shape, direction of motion of the fluid, and the lubrication area.[6] This anisotropic wetting property is of great interest for a broad range of applications such as liquid transportation,[7,8] self-cleaning coatings,[9,10] liquid-harvesting, and designs of smart devices.[11–14]

Despite anisotropic wetting being new to surface engineering, it has long existed in nature and been utilized by numerous plants and animals to realize diverse functions. These functions—for instance, fog-harvesting by spider silk, some beetles, and cacti,[15–17] directional water repelling by butterflies,[18] and one-dimensional water-directing properties of plant leaves[19]—enable their adaptation to their living environment and promote their survival. In these cases, such surfaces often comprise micro/nanoscale features, arranged directionally to produce direction-dependent wetting and liquid adhesion. The ingenious designs of biological surfaces come through years of evolution and species selection, inspiring the fabrication of artificial surfaces with anisotropic wettability.

Anisotropic wettability of surfaces is generally derived from gradients in chemistry[20,21] and surface features,[22–25] or the asymmetric asperities.[26–29] For the cases of surfaces with direction-dependent gradients in their chemical and structural features, motion of droplets is driven by the inhomogeneous surface free energy; alternatively, continuous motion is interrupted by abrupt surface roughness, resulting in a variation of contact angles in different directions. Whereas on the surfaces with asymmetric asperities, liquid slides or spreads spontaneously in one dimension because no changes of surface

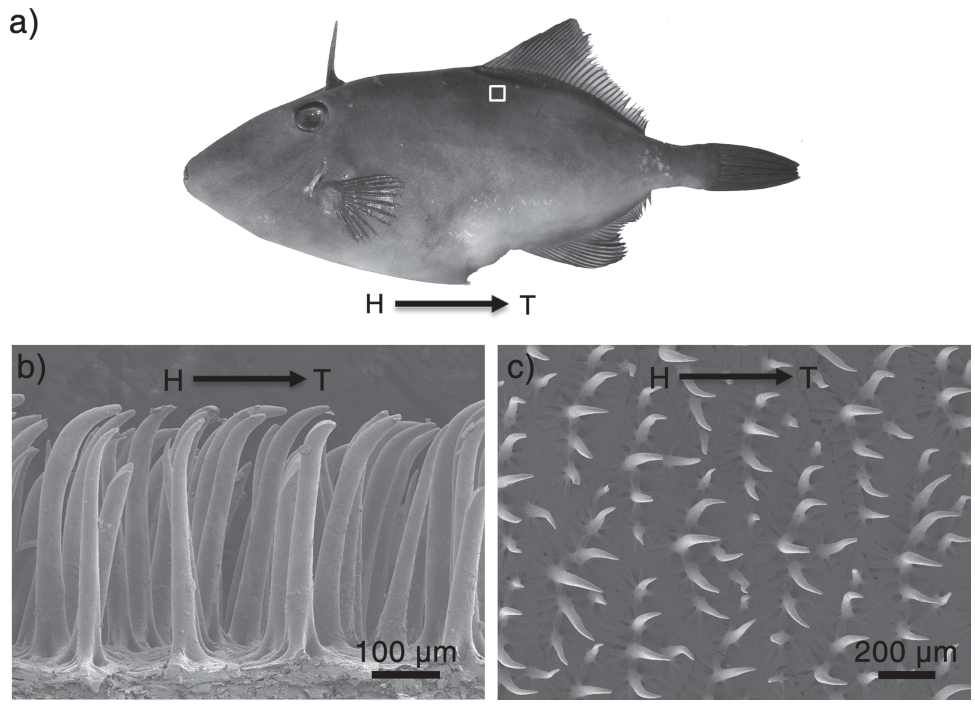

Figure 1. a) Photo of filefish *N. septentrionalis*. The arrow directing from head (H) to tail (T) indicates the oriented direction of hook-like spines SEM images of fish skin from the marked area in (a), showing b) a side-view and c) a top-view, show the hook-like microspines.

energy are introduced. Therefore, surfaces with asymmetric asperities displaying dynamic anisotropic wetting properties as opposed to static ones are rather meaningful for continuous direction of liquids. Until now, existing anisotropic wetting surfaces have succeeded in one-dimensional water directing and spreading. However, challenges are still encountered in driving an organic liquid that has a totally different wetting behaviour from water due to a lower surface tension. Practical, oil-wettable surfaces, especially in a three-phase water/oil/solid system, deeply relate to broad applications including water/oil separation, self-cleaning and oil-repellant coatings, and microfluidics.[30–35] To meet the ever-growing demand in these areas, it is urgent to explore surfaces with designable anisotropic oil wettability.

Our recent research may throw a light on the exploration of anisotropic underwater oleophobic surfaces. We found a kind of filefish *Navodon septentrionalis* (*N. septentrionalis*) which can swim in oil-spilled sea areas with oil directionally rolling off its skin from head to tail. To the best of our knowledge, such anisotropic oleophobicity on surfaces has not been found and reported until now. Herein, we reveal the oriented microscale features of the *N. septentrionalis* skin which result in the anisotropic underwater oleophobicity and propose a facile strategy to fabricate surfaces with this unique wettability. Following this proposed processing strategy, we reproduce anisotropic oleophobic surfaces both by mimicking biological microtextures on polydimethylsiloxane (PDMS) layers through soft lithography, and we establish oriented oblique features on polyacrylic acid (PAA) grafted commercial cloth. The hydrophilicity of the surface material and the anisotropic microstructures are proposed as two main factors in achieving anisotropic underwater oleophobicity. We anticipate our approach will be helpful in organic liquid handling and transportation, spill-oil collection, and the repellant coatings of ship hulls and oil pipelines.

2. Result and Discussion

2.1. Anisotropic Underwater Oleophobicity of *N. Septentrionalis* Skin

The filefish *N. septentrionalis*, primarily found in the Chinese and Japanese sea area of the Northwestern Pacific, has sandpapery bony skin instead of common flaky scales seen on other fish (**Figure 1**a).[36] In oil-spilled sea areas, *N. septentrionalis* is free from oil contamination. Moreover, we found that oil droplets tend to roll off along a head-to-tail (HT) direction, but tend to pin in the opposite direction (TH direction), motivating our further exploration. This anisotropic oil repellence may endow the filefish with directional easy-cleaning in oil spilled seawater, meanwhile avoiding accumulation of oil at its head.

N. septentrionalis skins feature visible hook-like spines throughout, which usually cause damage to fishing nets and sometimes even cause the injury of fishermen. This problem plagued the commercial exploitation of the fish until the 1970s. Since many previous studies have shown the crucial role of micro/nanoscale surface textures in the unique wetting properties of biological surfaces, we studied the detailed structure of this *N. septentrionalis* skin. With the aid of a scanning electron microscope (SEM), the hook-like spines and their arrangement on the filefish skin are clearly seen. Figure 1b shows the

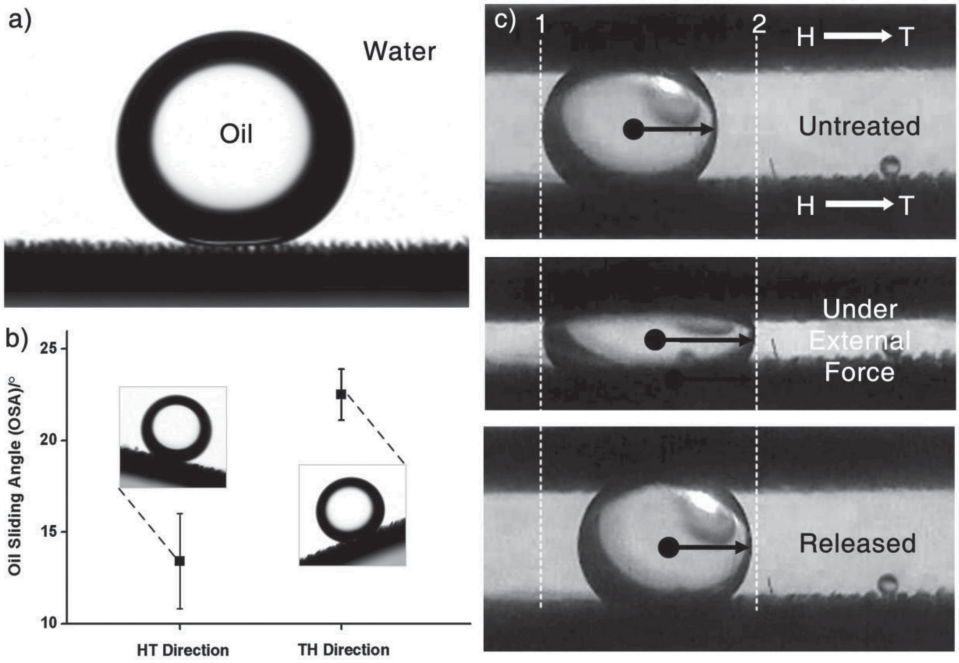

Figure 2. Anisotropic underwater oleophobicity of *N. septentrionalis* skin. a) The underwater oil contact angle (OCA) on fish skin is 156.1 ± 1.8°. b) Chart of anisotropic oil sliding angle (OSA) on the skin of *N. septentrionalis*. Along the HT direction, OSA is 13.4 ± 2.6°, while along the TH direction the OSA is 22.5 ± 1.4°. c) Anisotropic oil movement on fish skin under external force. The photos show the locations and shapes of oil droplets in an untreated state, under external force, and when released during one cycle of this force–release process. The centers of the oil droplets and directions of motion are respectively marked by black dots and arrows.

typical topography of the filefish skin from a side view. Each spine is 383.7 ± 17.6 μm high, 51.6 ± 5.4 μm wide (mean ± standard deviation, n = 10), curving at the tips and uniformly orienting towards the fish's tail (marked as the HT direction). These hook-like spines array in lines and each row of spines is more than 100 μm apart. Notably, the aspect ratio of spines is as high as 8, probably leading to the macroscopic roughness of filefish skin.

It is generally accepted that surface roughness contributes significantly to enhancing liquid repellence.[37,38] In our study, we found that the tough hook-like spines on *N. septentrionalis* help to maintain stable underwater superoleophobicity, which is even free from the disturbance of external forces and slight structural damage. **Figure 2**a shows the underwater superoleophobicity of *N. septentrionalis* skin with an oil contact angle (OCA) of up to 156.1 ± 1.8° (mean ± standard deviation, n = 5), indicating a limited attraction between the oil and the skin. Underwater oleophobicity has already been found on several surfaces of aquatic creatures, and the fabrication of such surfaces relies on the employment of high-surface-energy materials, further enhanced by surface roughness.[39–42] This is also true for the case of *N. septentrionalis*. Its skin is reported to be composed of high surface-energy organics such as collagen, explaining the underwater oleophobicty via its chemical composition.[43] Furthermore, the closely arrayed hook-like spines increase the performance of underwater oleophobicty by tightly interlocking plenty of water molecules into the spaces of each spines. The trapped water molecules function as a repulsive liquid to protect fish skin from oil invasion on water/oil/solid interface, in the same way that trapped air contributes to the hydrophobicity in the Cassie model.[38] Simultaneously, the high aspect ratio and remarkable hardness of spines optimize the stability of the underwater oleophobicity under external forces or slight surface damage, to easily maintain adequate trapped water between the residual unstrained or unbroken parts.

In addition to stable underwater oleophobicity, a unique oil-wetting anisotropy is found in the *N. septentrionalis* skin system which hasn't been observed on other biological surfaces. This anisotropic underwater oleophobicity is reflected in inhomogeneous liquid movement in opposite directions, being characterized by the measurement of oil sliding angle (OSA) and recorded by CCD camera. A previous study demonstrated that directional shedding of droplets is related to the volume of liquid.[19] For the droplet with big volume, the sliding angles of droplet in opposite directions will decrease simultaneously due to the influence of gravity. The degree of wetting anisotropy of a surface may hinder this estimate. Therefore, we only measured the OSA for a droplet of 3 μL, and the result is shown in the chart of Figure 2b. Along the HT direction, oil droplets rolled off fish skin at the angle of 13.4 ± 2.6°; while along the TH direction, the OSA is 22.5 ± 1.4°, which is approximately 9° larger. Interestingly, the preferential moving direction of oil fluid corresponds with the tilting orientation of hook-like spins on *N. septentrionalis* skin. As is usually observed on biological surfaces, anisotropic textured surfaces provide the basis for direction-dependent wettability. Therefore, we believe the curved tips of the spines drive the anisotropic motion of oil droplet, and the high-aspect-ratio of the spines enable the skin's exceptional oil repellence.

Since a shear force is generated as fish swim, we envision that a combination of the shear force and oriented microtextures will enhance the capability of self-cleaning. Actually, we found the external force in perpendicular to the filefish body also cause the anisotropic locomotion of oil droplet. Aiming to clearly illustrate the process, we used a CCD camera to record underwater oil movement on *N. septentrionalis* skin driven by external forces. As shown in Figure 2c, an oil droplet was placed between two pieces of fresh *N. septentrionalis* skin, which were finely pasted on glass slides. The oriented directions of the hook-like spines on both skin pieces were kept uniform, as indicated by arrows in the figure. For the convenience of analysis and explanation, the boundaries of the oil drop have been marked as 1 and 2 at the receding and advancing edges, respectively. It was found that, when the glass slides were pressed together, the spherical oil droplet stretched into an ellipsoid with boundary 1 pinning and boundary 2 advancing. After withdrawing the force, the oil droplet was released and reverted to its original shape, moving ahead at boundary 1 but holding at boundary 2. In this way, the oil droplet advances unidirectionally along the oriented spines without loss in volume during cycles of force and release. Moreover, this directional oil transportation can be made continuous by repeating this process, due to the low oil adhesion of the *N. septentrionalis* skin.

According to previous explorations, the retention force that impedes the liquid movement is not equal in different directions on a surface with asymmetric features.[44] On a surface with a homogeneous chemical composition the contact angle hysteresis is constant, and the difference in the values of the retention forces for opposite directions increases with the degree of topographic asymmetry. Moreover, liquids can advance only if the contact line is able to reach the next row of spines, meaning that the liquid is prone to propagating along the slant direction of the topographic features.[27] In this sense, the oil droplet prefers to stretch and advance unidirectionally along the oriented direction of the hook-like spines, displaying anisotropic oleophobicity on a macroscopic scale. Notably, there is no loss of oil during the transportation, indicating its potential application for long-distance oil transportation.

2.2. Preparation and Surface Characterization of Artificial *N. Septentrionalis* Skin

The anisotropic superoleophobic system of *N. septentrionalis* skin that relies on the combination of oriented microtextures and hydrophilic materials offers ideas to design surfaces for oil transportation with high efficiency. We synthesized a replicate surface of *N. septentrionalis* skin via soft lithography. Soft lithography is a superior choice in terms of simplicity and wide applicability for duplicating varied biological surfaces which have complex surface topography.[45–47] In our approach, we employed a widely used polymer in soft lithography, polydimethylsiloxane (PDMS, SYLGARD 184), as a moulding material and the fabrication progress of artificial fish skin is illustrated in **Figure 3**a. Briefly, the *N. septentrionalis* skin was firstly finely rinsed and then gradient dehydrated to enhance its hardness, to avoid distortion during PDMS moulding. Subsequently, the pre-treated *N. septentrionalis* skin was used as the template for a negative PDMS mould which then self-moulded to fabricate the positive replica of oriented hook-like spines. For the convenience of peeling the positive replica, the negative

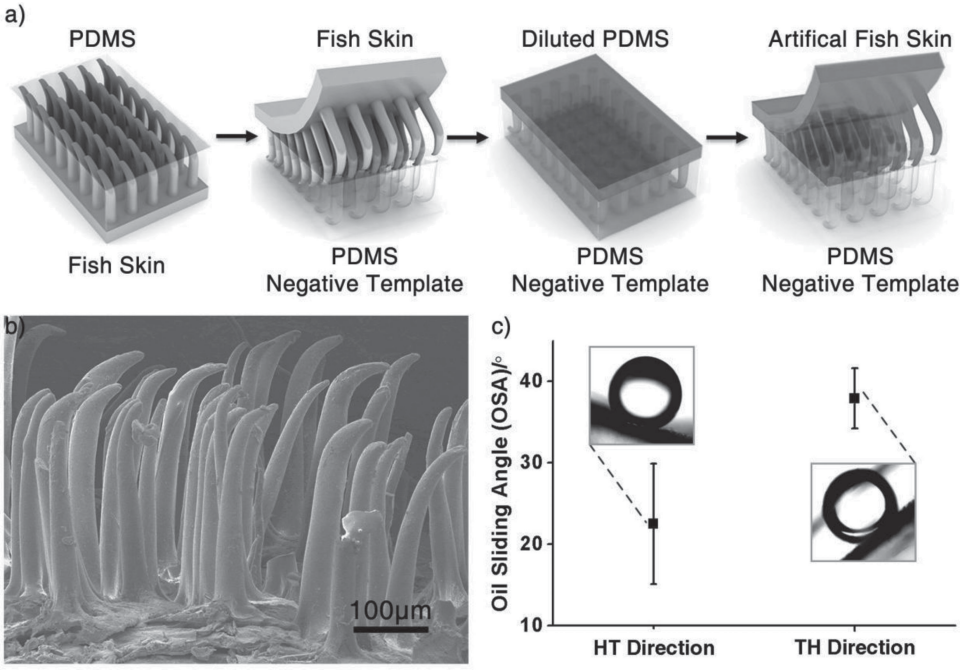

Figure 3. a) Illustration of the fabrication process for artificial fish skin. b) SEM image of artificial fish skin fabricated by toluene-diluted PDMS. c) Chart of anisotropic OSA on oxygen-plasma-treated PDMS fish skin. The OSA values are 22.5 ± 7.3° along the HT direction and 38.7 ± 3.7° along the TH direction.

PDMS template is first grafted with fluoride molecules (heptadecafluorodecyltrimethoxysilane) before moulding. The pure PDMS material is too fragile to maintain the high-aspect-ratio microstructures and fails to replicate of curve tips of spines. To overcome this drawback, PDMS is usually diluted with an organic solution such as silicon oil or toluene.[48,49] Accordingly, we diluted the pre-polymer of PDMS with toluene in the proportions 4:1 by weight to fabricate refined structures. After curdling at 80 °C for 4 h, the replica of fish skin was obtained. It successfully reproduced the biological structures of spines with integrity of shape and curvature. From the above analysis of biological fish skin, the premise of achieving underwater oleophobicity is the hydrophilicity of surface composition, namely, the high surface energy of the material. However, PDMS is typically a material with low surface energy, resulting in the weak interlocking of water to repel oil.[50] To solve this, the PDMS artificial fish skin was treated with oxygen plasma to expose polar functional groups, allowing the formation of hydrogen bonds with water molecules.[51–53] As a result, the PDMS artificial fish skin displayed oleophobicity underwater with an OCA of 143 ± 2.1°.

This oxygen-plasma-treated artificial fish skin also shows a remarkable anisotropy of oil repellence, with a large OSA difference of up to 15° between opposite directions (Figure 3c). In the HT direction, the oil droplet rolled at 22.5 ± 7.3°, but nearly stays still even at a large tilt angle until reaching the OSA of 37.9 ± 3.7° in the opposite direction. However, a significant difference of OSA on biological and artificial surfaces was also observed. According to the OSA values in both directions, the oil droplet can more easily roll off biological fish skins than the PDMS artificial ones. This wettability difference probably results from the weaker underwater oleophobicity of oxygen-plasma-treated PDMS, indicating the importance of the chemical composition of processed surfaces.

2.3. Strategy for Fabricating Anisotropic Underwater Oleophobic Surfaces

Drawn from the exploration above, bioinspired anisotropic oleophobic surfaces can be prepared based on two criteria: the hydrophilicity of the surface, which ensures that abundant water molecules bond to the surfaces and provide a repulsive force against oil immersion; the asymmetric microtextures, which drive the anisotropic motion of fluid on the surfaces, and the degree of topographic asymmetry, which determines the imbalance of oleophobicity in different directions. Therefore, the anisotropy of underwater oleophobicity can be tailored by adjusting the tilt angle of the spines, combined with hydrophilic treatment of the surface. This process is further demonstrated by processing a commercial cloth corduroy, demonstrating the applicability of this method to engineering large-scale surfaces. The corduroy is composed of nearly 1200 μm-long cloth fibres that mimic the high-aspect-ratio spines on filefish skin. In our approach, the corduroy was first ironed uni-directionally 5, 10, 20, and 50 times, making the cloth fibre tilt increasingly. **Figure 4**b shows the SEM images and the tilting conditions

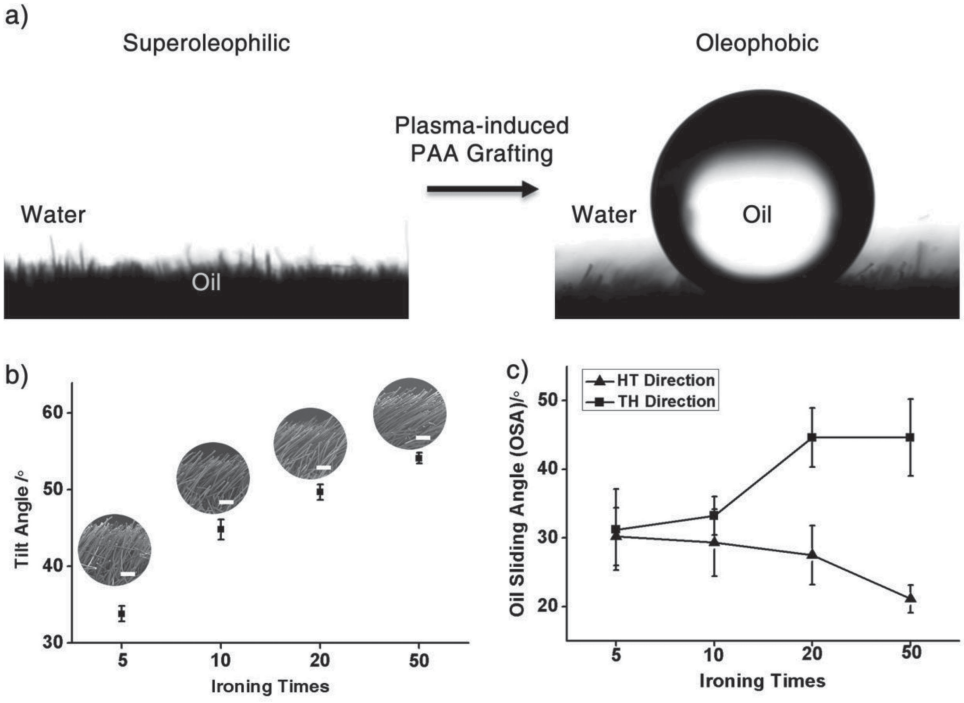

Figure 4. The anisotropic underwater oleophobicity of tilted corduroy. a) The OCA of untreated (left) and PAA-grafted (right) corduroy. PAA modification changes the wettability of corduroy from superoleophilic to oleophobic. The OCA of PAA-grafted corduroy is 147.4 ± 2.8°. b) The tilt angle of cloth fibres increases with ironing times. The inset SEM images show the oblique cloth fibre after the corresponding ironing times. Scale bars in SEM images stand for 200 μm and the error bar is the standard error of the mean (N = 50). c) The anisotropic wetting phenomenon is influenced by the tilt angle of the cloth fibres. The chart exhibits the OSA on ironed cloth samples along the HT and TH directions after plasma-induced grafting of PAA. Asymmetric microstructures lead to the differences of OSA in the two directions.

of cloth fibres after ironing. Such oblique microscale fibres function as the oriented, curved tips of the spines on the fish skin, impelling the anisotropic fluidic motion. Commercial corduroy, due to its chemical composition, is superoleophilic, hardly meeting the needs to repel oil underwater. To address this limitation, a hydrophilic polymer, polyacrylic acid (PAA) was grafted onto oblique cloth fibres by plasma-induced graft polymerization.[54,55] PAA is a weak polyelectrolyte containing carboxylic groups, which stretches its conformation and forms intermolecular hydrogen bonds with water molecules when the pH is above its pK_a of 4.7.[56] Therefore, it acts hydrophilic in deionized water, making the grafted corduroy oleophobic under water. Figure 4a shows the wettability conversion of corduroy before and after the plasma-induced PAA graft, with the OCA changing from 0° to 147.4 ± 2.8°.

With increasing tilt angle of the cloth fibres, the as-prepared surfaces exhibit a remarkable increase of wetting anisotropy in one dimension, signified by the corresponding differences of OSA along and against the tilt direction. Especially in the case of 50-times-ironed sample, of which the tilt angle is up to 54.1 ± 0.7°, the OSA along the tilt orientation is approximately 20° larger than that in the opposite direction (Figure 4c). It means that the oil droplet nearly sticks in one direction but flows freely in the opposite direction. However, as for the least tilted sample which was ironed 5 times, there is nearly no directional difference of OSA observed. Furthermore, we found, on the 50-times-ironed sample, oil droplets can be directed along the oriented microstructures under external force, just like the phenomenon previously observed on biological fish skin. As shown in **Figure 5**, the oil droplet moved forward unidirectionally after one force–release cycle. This proves that the anisotropy of underwater oleophobicity can be controlled by adjusting the degree of asymmetry of microtextures.

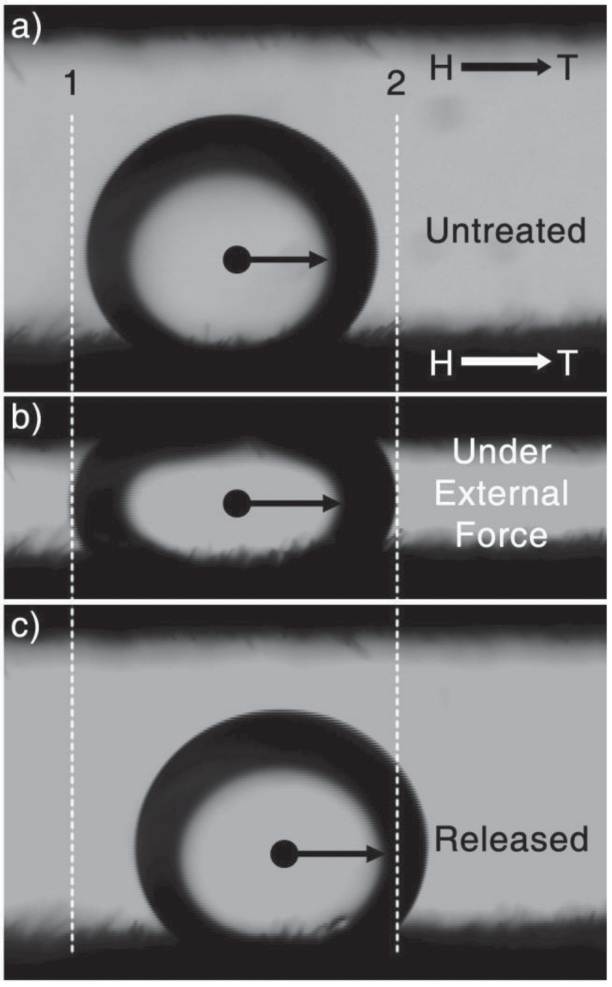

Figure 5. Directional oil movement under external forces on PAA-grafted corduroy. Panels (a) to (c) show the oil droplet in an untreated state, forced, state and released state, respectively. The dotted lines 1 and 2 indicate the receding edge and advancing edge of the oil droplet under external force, respectively.

3. Conclusions

We revealed the unique anisotropic underwater oleophobicity of filefish *N. septentrionalis* skin which results from the anisotropic microtexture-featured, oriented hook-like spines. Inspired by it, we successfully fabricated an artificial fish skin with similar anisotropic wetting behaviour by mimicking the hook-like spines on a PDMS layer and subsequent oxygen plasma treatment. Drawn from our exploration, the anisotropic underwater oleophobicity can be achieved by two main factors: the anisotropic microtextures on the surface and hydrophilic surface composition. Accordingly, the fabrication strategy was then proved on PAA-grafted cloth corduroy, on which the wetting anisotropy is controlled by the tilt angles of cloth fibres.

Our approach is just a simple demonstration of this bioinspired principle, however, it provides powerful evidence to support its applicability in overcoming the challenges of manufacturing large-area anisotropic underwater oleophobic surfaces for commercial use. Since the high-surface-energy materials, acquired via this fabrication principle, are abundant and commercially available and can even be achieved by surface treatments such as polymer grafts, surfaces with anisotropic underwater oleophobicity can be fabricated by processing the anisotropic microtextures. Meanwhile, the wetting anisotropy of as-prepared surfaces can also be controlled by changing the structural details. This means that, in practice, materials and anisotropic microstructures of surfaces can be adjusted to satisfy the varied needs of the applied conditions including durability, environmental friendliness, fabricating expense, and process complexity. We anticipate that filefish-inspired anisotropic underwater oleophobic surfaces will benefit the development of surface designs in applications of underwater organic fluid directing, oil transport, high-efficient oil collection, and self-cleaning coatings for ship hulls and oil pipelines.

4. Experimental Section

Instruments and Characterization: SEM images were obtained using a field-emission scanning electron microscope (JSM-7500F, Japan) to characterize surface topography. Oil contact angles (OCA) and oil sliding angles (OSA) were measured on an OCA20 machine (Data-Physics, Germany) at ambient temperature. All the OCA and OSA measurements were carried out with water and oil phases being referenced against

1,2-dichloroethane. The larger density of 1,2-dichloroethane compared to water facilitates underwater tests of sliding angles. The samples are immersed in deionized water and no air bubbles were allowed to remain on testing surfaces. During the measurements of oil wettability, the needle of the microsyringe was firstly immersed into the water, and then 3 μL oil was dispensed and slightly shaken down onto the surface. The average of the OCA and OSA appearing in the main text is from the values measured on 5 different places of the tested surfaces. All the testing data of *N. septentrionalis* skin was acquired on untreated skin samples.

Pre-treatment of Fish Skins: The *N. septentrionalis* was acquired in a seafood market of Dalian, China. The skins of *N. septentrionalis* were rinsed thoroughly in water and then the gradient dehydrated by 50 vol%, 75 vol%, 90 vol%, 95 vol%, and 100 vol% ethanol solution under ultrasonication for 10 min. Gradient dehydration promoted the hardness of filefish skin, protecting it from distortion and damage during PDMS curing.

External Force-Induced Movement Experiments: Untreated skins of *N. Septentrionalis* were pasted onto glass slides. One piece of glass slide was fastened on the bottom of a water pool and the other was fixed onto an iron support stand. The surface orientation of two pieces of *N. septentrionalis* skin was kept in the same direction. A CCD camera was used to record the shape distortion and movement of oil drops while applying and withdrawing an external force onto the glass slide. The external force-induced experiments were carried out according to the same process on PAA-grafted corduroy, which was directionally ironed 50 times.

Fabrication of Artificial Topography of Fish Skins: The fabrication process is illustrated in Figure 3. Polydimethylsiloxane (Sylgard 184) precursor was mixed with a curing agent in the proportion of 10:1 by weight. The PDMS mixture was put into a centrifuge to remove air bubbles (3000 rpm, 5 min). Then the mixture was poured onto the gradient dehydrated skins of *N. septentrionalis*. To insure the fine replicating of the fish skins, the remaining air bubbles between the PDMS and fish skins were removed in a vacuum chamber. After heating at 60 °C for 4 h, the fish skins were carefully peeled along the HT direction to avoid breaking the tips of the structure. A PDMS negative template was then grafted using fluoride molecules (heptadecafluorodecyltrimethoxysilane) in a decompressed environment at room temperature for 24 h and then heated at 80 °C for 3 h. The fluoride molecules decrease the surface energy of PDMS negative templates and facilitate the peeling of positive microstructures. Toluene-diluted PDMS (PDMS:toluene = 4:1 w/w) was poured on the fluorinated negative template and then it was cured at 80 °C for 2 h. The artificial PDMS fish skin was also carefully peeled off the negative template along the HT direction. The PDMS artificial fish skin was put in an oxygen plasma reactor (Suzhou Omega Machinery Electronic Technology Co., Ltd., DT-03) and went through a glow discharge at 100 W for 5 min. After oxygen-plasma treatment, silanol group (–SiOH) is exposed on the surface, making the surface hydrophilic for hours.

Preparation of Unidirectional Tilted Corduroy: Corduroy cloth was cut into 2 cm × 3 cm pieces and pasted onto glass sides. The iron used was a household one, purchased from a supermarket. Before ironing, the pieces of corduroy were sprayed with water and the electric iron was pre-heated to around a stable 200 °C. Corduroy pieces were ironed in a single direction 5, 10, 20, and 50 times under steam mode of the electric iron. The tilt angle of the cloth fibre of each sample was calculated from 50 fibres from 10 SEM pictures and the error bars refer to the standard error of the mean.

Plasma-Induced PAA Polymerization on Corduroy: The ironed corduroy was treated with plasma-induced grafting in the vapor phase of distilled acrylic acid (AAc) to ensure its stable, long-term hydrophilicity. The details of the preparation method can be found in our previous report.[55] In brief, the unidirectionally ironed corduroy samples were put in the plasma-induced grafting reactor (Suzhou Omega Machinery Electronic Technology Co., Ltd., DJ-01). The chamber was evacuated and then filled with argon at 50–70 Pa for 15 min. After a glow discharge at 20 W for 30 min, acrylic acid monomer was pumped into the grafting reactor at a pressure of 300–600 Pa, maintained for about 20 min.

Acknowledgements

Y. Cai and L. Lin contributed equally to this work. The authors acknowledge the financial support from the Chinese National Research Fund for Fundamental Key Projects (2012CB933800, 2012CB934100), the National Natural Science Foundation (21175140, 21121001, 91127025), and the Key Research Program of the Chinese Academy of Sciences (KJZD-EW-M01). Thanks to Dr. Meihua Jin and Dr. Xiuling Li for providing *N. septentrionalis* used in experiments.

Received: June 14, 2013
Revised: July 2, 2013
Published online: September 13, 2013

[1] C. W. Extrand, S. I. Moon, P. Hall, D. Schmidt, *Langmuir* **2007**, *23*, 8882.
[2] R. Wang, K. Hashimoto, A. Fujishima, M. Chikuni, E. Kojima, A. Kitamura, M. Shimohigoshi, T. Watanabe, *Nature* **1997**, *388*, 431.
[3] J. Z. Wang, Z. H. Zheng, H. W. Li, W. T. S. Huck, H. Sirringhaus, *Nat. Mater.* **2004**, *3*, 171.
[4] T.-S. Wong, S. H. Kang, S. K. Y. Tang, E. J. Smythe, B. D. Hatton, A. Grinthal, J. Aizenberg, *Nature* **2011**, *477*, 443.
[5] B. Zhao, J. S. Moore, D. J. Beebe, *Science* **2001**, *291*, 1023.
[6] D. Xia, L. M. Johnson, G. P. López, *Adv. Mater.* **2012**, *24*, 1287.
[7] V. Jokinen, M. Leinikka, S. Franssila, *Adv. Mater.* **2009**, *21*, 4835.
[8] A. Shastry, M. J. Case, K. F. Böhringer, *Langmuir* **2006**, *22*, 6161.
[9] N.-R. Chiou, C. Lu, J. Guan, L. J. Lee, A. J. Epstein, *Nat. Nanotechnol.* **2007**, *2*, 354.
[10] H. Zhao, K.-Y. Law, *Langmuir* **2012**, *28*, 11812.
[11] K. Ichimura, S.-K. Oh, M. Nakagawa, *Science* **2000**, *288*, 1624.
[12] G. Qing, X. Wang, H. Fuchs, T. Sun, *J. Am. Chem. Soc.* **2009**, *131*, 8370–8371.
[13] G. Qing, T. Sun, *Adv. Mater.* **2011**, *23*, 1615–1620.
[14] C. Li, Y. Zhang, J. Ju, F. Cheng, M. Liu, L. Jiang, Y. Yu, *Adv. Funct. Mater.* **2012**, *22*, 760.
[15] H. Bai, J. Ju, Y. Zheng, L. Jiang, *Adv. Mater.* **2012**, *24*, 2786.
[16] J. Ju, H. Bai, Y. Zheng, T. Zhao, R. Fang, L. Jiang, *Nat. Commun.* **2012**, *3*, 1247.
[17] A. R. Parker, C. R. Lawrence, *Nature* **2001**, *414*, 33.
[18] Y. Zheng, X. Gao, L. Jiang, *Soft Matter* **2007**, *3*, 178.
[19] P. Guo, Y. Zheng, C. Liu, J. Ju, L. Jiang, *Soft Matter* **2012**, *8*, 1770.
[20] H. Gau, S. Herminghaus, P. Lenz, R. Lipowsky, *Science* **1999**, *283*, 46.
[21] M. Morita, T. Koga, H. Otsuka, A. Takahara, *Langmuir* **2004**, *21*, 911.
[22] J. Y. Chung, J. P. Youngblood, C. M. Stafford, *Soft Matter* **2007**, *3*, 1163.
[23] Y. Zhao, Q. Lu, M. Li, X. Li, *Langmuir* **2007**, *23*, 6212.
[24] D. Xia, S. R. J. Brueck, *Nano Lett.* **2008**, *8*, 2819.
[25] T. Wang, X. Li, J. Zhang, X. Wang, X. Zhang, X. Zhang, D. Zhu, Y. Hao, Z. Ren, B. Yang, *Langmuir* **2010**, *26*, 13715.
[26] T.-i. Kim, K. Y. Suh, *Soft Matter* **2009**, *5*, 4131.
[27] K.-H. Chu, R. Xiao, E. N. Wang, *Nat. Mater.* **2010**, *9*, 413.
[28] W. Wu, L. Cheng, S. Bai, Z. L. Wang, Y. Qin, *Adv. Mater.* **2012**, *24*, 817.
[29] N. A. Malvadkar, M. J. Hancock, K. Sekeroglu, W. J. Dressick, M. C. Demirel, *Nat. Mater.* **2010**, *9*, 1023.
[30] K. Tsujii, T. Yamamoto, O. Tomohiro, S. Shibuichi, *Angew. Chem. Int. Ed.* **1997**, *36*, 1011.
[31] Q. Xie, J. Xu, L. Feng, L. Jiang, W. Tang, X. Luo, C. C. Han, *Adv. Mater.* **2004**, *16*, 302.
[32] A. Tuteja, W. Choi, M. Ma, J. M. Mabry, S. A. Mazzella, G. C. Rutledge, G. H. McKinley, R. E. Cohen, *Science* **2007**, *318*, 1618.

[33] H. Wang, Y. Xue, J. Ding, L. Feng, X. Wang, T. Lin, *Angew. Chem. Int. Ed.* **2011**, *50*, 11433.
[34] H. Jin, M. Kettunen, A. Laiho, H. Pynnönen, J. Paltakari, A. Marmur, O. Ikkala, R. H. A. Ras, *Langmuir* **2011**, *27*, 1930.
[35] L. Cao, T. P. Price, M. Weiss, D. Gao, *Langmuir* **2008**, *24*, 1640.
[36] G.-B. Xu, Y.-S. Tian, X.-L. Liao, S.-L. Chen, *Conserv. Genet.* **2009**, *10*, 1181.
[37] R. N. Wenzel, *Ind. Eng. Chem.* **1936**, *28*, 988.
[38] A. B. D. Cassie, S. Baxter, *Trans. Faraday Soc.* **1944**, *40*, 546.
[39] M. Liu, S. Wang, Z. Wei, Y. Song, L. Jiang, *Adv. Mater.* **2009**, *21*, 665.
[40] Y. C. Jung, B. Bhushan, *Langmuir* **2009**, *25*, 14165.
[41] V. Hejazi, M. Nosonovsky, *Langmuir* **2011**, *28*, 2173.
[42] X. Liu, J. Zhou, Z. Xue, J. Gao, J. Meng, S. Wang, L. Jiang, *Adv. Mater.* **2012**, *24*, 3401.
[43] M. Ahmad, S. Benjakul, M. Ovissipour, T. Prodpran, *Food Chem.* **2011**, *127*, 508.
[44] C. W. Extrand, *Langmuir* **2007**, *23*, 1867.
[45] M. Sun, C. Luo, L. Xu, H. Ji, Q. Ouyang, D. Yu, Y. Chen, *Langmuir* **2005**, *21*, 8978.
[46] W. S. Beh, I. T. Kim, D. Qin, Y. Xia, G. M. Whitesides, *Adv. Mater.* **1999**, *11*, 1038.
[47] G. Zhang, J. Zhang, G. Xie, Z. Liu, H. Shao, *Small* **2006**, *2*, 1440.
[48] H. Kang, J. Lee, J. Park, H. H. Lee, *Nanotechnology* **2006**, *17*, 197.
[49] N. Koo, M. Bender, U. Plachetka, A. Fuchs, T. Wahlbrink, J. Bolten, H. Kurz, *Microelectron. Eng.* **2007**, *84*, 904.
[50] R. F. Brady, I. L. Singer, *Biofouling* **2000**, *15*, 73.
[51] M. Morra, E. Occhiello, R. Marola, F. Garbassi, P. Humphrey, D. Johnson, *J. Colloid Interface Sci.* **1990**, *137*, 11.
[52] H. Hillborg, J. F. Ankner, U. W. Gedde, G. D. Smith, H. K. Yasuda, K. Wikström, *Polymer* **2000**, *41*, 6851.
[53] A. Oláh, H. Hillborg, G. J. Vancso, *Appl. Surf. Sci.* **2005**, *239*, 410.
[54] S.-D. Lee, G.-H. Hsiue, P. C.-T. Chang, C.-Y. Kao, *Biomaterials* **1996**, *17*, 1599.
[55] X. Hou, Y. Liu, H. Dong, F. Yang, L. Li, L. Jiang, *Adv. Mater.* **2010**, *22*, 2440.
[56] J. W. Lee, S. Y. Kim, S. S. Kim, Y. M. Lee, K. H. Lee, S. J. Kim, *Appl. Surf. Sci.* **1999**, *73*, 113.